

Zirconium, cerium and yttrium on Ti cathodes for evolution of H_2 in an acid electrolyte

S. Voskanyan¹, A. Tzanev¹, N. Shroti², G. Pchelarov¹, K. Petrov^{1*},

¹*Institute of Electrochemistry and Energy Systems, Bulgarian Academy of Sciences, G. Bonchev Str., Bl. 10, 1113, Sofia, Bulgaria*

²*Department of Chemical Engineering, University of Patras, GR 26504 Patras, Greece*

Received December 16, 2014, Revised May 20, 2015

Zirconium, cerium and yttrium electrodes were prepared by electrochemical deposition and were studied as catalysts for hydrogen evolution. Cathodes were prepared from $ZrCl_4$ & $CeCl_3 \cdot 7H_2O$ & $YCl_3 \cdot 6H_2O$ on Ti-felt. The hydrogen evolution reaction was investigated in acid solutions: 1M or 4.5 M H_2SO_4 (liquid) and PBI membranes with phosphoric acid at room and elevated temperatures. The morphology and the microstructure of the electrodes were characterized by SEM and X-ray diffraction. The electro catalytic activity was evaluated based on steady-state polarization curves, Tafel plots and electrochemical impedance spectroscopy. It was shown that the electro catalytic activity of the prepared electrodes depends on the morphology and microstructure of the porous electrode. It has a low charge transfer resistance, and high exchange current density. Its electro catalytic activity was studied in the temperature interval, $t^\circ = 25^\circ$ to $160^\circ C$.

Keywords: electrolysis, H_2 evolution.

INTRODUCTION

Water electrolysis is a clean method for the production of highly pure hydrogen in large quantities. Furthermore, water electrolysis can utilize energy from renewable sources. However, the main problem with electrolytic hydrogen is the high cost of the consumed energy. Increasing the temperature to values of 150 – $250^\circ C$ should result in a higher efficiency yet lower cost of the hydrogen produced.

To make this technique more efficient and economical, new catalysts and electrode materials have to be developed.

Among many tested catalysts Zr/Ce/Y has a special place, especially for reactions at high temperatures [1]. The relative inefficiencies of the cathodes and the need for more efficient electro-catalysts that perform well at higher temperatures have directed research efforts for some time [2]. The Brewer inter-metallic bonding theory [3] linked the electronic configuration and the crystal structure for both individual transition elements and their inter-metallic phases and alloys. At the same time the Brewer inter-metallic bonding model and the theory of electro-catalysis for hydrogen electrode reactions (HELRL) were consolidated [4]. In the past the utilization of Ti has shown varied

results dependent on the material characteristics. The H_2 absorbed per 100 g of metal was reported to be: 50 – 100 cm^3 for compact metal, 280 – 330 cm^3 for metal in sponge form and 300 – 5300 cm^3 for Ti powder [5]. At the turn of this century CeO_2 attracted much attention for its catalytic applications, ability to decontaminate noxious compounds from gases and degrade organic pollutants in wastewater through catalytic wet oxidation [6]. A key property of ceria–zirconia oxides in their role as catalysts or catalyst supports is their ability to exchange lattice oxygen with reactants, referred to as Oxygen Storage Capacity (OSC) [7]. A more comprehensive search for Zr/Ce/Y catalysts lead to a US patent filed in 2007 entitled “Cyclic catalytic upgrading of chemical species using metal oxide materials” that lists a plethora of transition metal oxide materials promising as catalysts [8]. In Solid Oxide Electrolysis Cells (SOEC) the most common electrolyte material is a dense ionic conductor consisting of ZrO_2 doped with 8 mol% of Y_2O_3 (YSZ) [9]. More recently, 15% CeO_2/ZrO_2 and 13% CeO_2/YSZ catalysts were prepared by incipient wetness impregnation of the corresponding oxides (25 g), in three successive steps, using an aqueous solution of $Ce(NO_3)_3 \cdot 6H_2O$ [10]. The structural and chemical features of the supported ceria imprinted by such treatments allow for obtaining a material of outstanding reducibility at low temperatures. Details of the chemical

* To whom all correspondence should be sent:
E-mail: kpetrov@bas.bg

reaction when O₂ reacts with H adatoms on rutile TiO₂ have been shown by high-resolution STM studies and DFT calculations. O₂ molecules react with H adatoms, leading to a series of intermediate H transfer reaction steps until the formation of water is complete [11].

In PEM electrolysis, a thin ($\approx 100\ \mu\text{m}$) perfluorosulfonate polymer membrane (PFS) is used as a solid electrolyte [12]. The commercial Nafion[®] membrane from Dupont[®] is ordinarily used due to its excellent chemical and thermal stability, mechanical strength, and high proton conductivity. However, using such membranes has disadvantages, namely operational temperature, cost and disposal. Their disposal can be expensive due to the contained fluorine in the backbone structure [13]. Research groups have been concentrating their efforts to make less expensive proton exchange membranes, but also focusing on improving their ion exchange characteristics and durability for PEM electrolysis. Nafion[®] membranes have been extensively studied in PEM fuel cells [14]. However, the hydration state of the membrane differs between fuel cell operation and electrolysis operation. During PEM fuel cell operation, the membrane is humidified by the gases and equilibrated with water vapor, whereas during the PEM electrolysis operation, the electrolyte membrane is exposed to the liquid phase of water and fully hydrated during water electrolysis [15].

The increase in the temperature of operation offers several advantages from thermodynamic, kinetic and engineering points of view. When the temperature is increased, the electrode kinetics will be enhanced and therefore the over-potentials will be reduced. If water reacts above 100 °C in the gaseous form, the electrolysis process will be thermodynamically less energy demanding. The reversible voltage of the electrolysis cell is 1.23 V at 25 °C, considerably higher than at 200 °C for steam water (1.14 V). Better membrane hydration and proton conductivity characteristics can also be obtained when the electrolysis system is pressurized. Hence, it would be important to develop membranes that can sustain a higher temperature of operation. In the last decades, PA doped poly[m-phenylene-bis(5,5'-benzimidazole)] (PBI) membranes have emerged as a promising PEM material for applications in fuel cells operating at temperatures of up to 200 °C [16], [17], [18]. The rigid aromatic backbone of these PBI membranes provides the necessary chemical and thermal stability. However, in PBI/PA systems, the proton conductivity is strongly dependent on the acid doping level [19], the PA concentration

together with the high temperature being responsible for a critical corrosion limiting condition for the overall system [20]. Which is a new polymeric membrane composed from an aromatic polyether containing pyridine units in the structure. This alternative type of polymeric material is composed from an aromatic polyether backbone containing main chain or side chain pyridine units, where the H₃PO₄ binds and is retained in the membrane matrix. Beyond their good mechanical and chemical properties the aforementioned membrane types have high glass transition temperatures (above 260°C) combined with high thermal stability up to 400°C. Doping of these poly-ethers with phosphoric acid resulted in materials with ionic conductivity in the range of 10⁻² S/cm as reported [21].

EXPERIMENTAL

Materials

Phosphoric acid-doped polymer electrolyte membranes were provided by Advent Technologies S.A[®]. The Ti felt with a thickness of 0.2 mm was supplied by “Bekaert metal fiber Co. Ltd.”. H₃PO₄ $\geq 85\%$ was purchased from Merck or Sigma Aldrich. All the chemicals were used as received unless otherwise noted.

Electrode preparation

Ti-felt was prepared according to a procedure described elsewhere [22]. ZrO₂-CeO₂-Y₂O₃ catalytic layers were electrodeposited on it. The process of electro deposition was carried out in a standard two-electrode electrochemical cell with a volume of 175 ml and a double jacket for water cooling. Pieces of Ti-felt were utilized as cathodes on which a triple system was deposited. Platinum covered Ti with an area 2.5 times larger than the cathode was used as the anode. The cathode was placed in the center of the cell between two anodes. The distance between the anodes was 4 cm.

In the process of electroplating a thin film electrolyte was used, containing ZrCl₄, pre-dissolved in ethyl alcohol, CeCl₃.7H₂O and YCl₃.6H₂O with concentrations given in Table 1. The electro deposition of thin catalytic films was carried out in the potentiostatic mode with continuous mechanical stirring of the solution. The high specific resistance of the electrolyte causes heating of the electrolyte during the electrolysis process, which requires its continuous cooling to temperatures of 10 to 12°C, found to be optimal in the preliminary experiments. After the electro deposition of thin catalytic films the samples were washed thoroughly with distilled water and dried.

Electrochemical testing

The cell employs a HER electrode (Zr, Y & Ce on Ti) and a hydrogen oxidation electrode (Pt/C, carbon/teflon gas diffusion layer, which was supported on carbon cloth provided by Advent technologies) working in a fuel cell mode, due to the high corrosion of the cell during oxygen evolution. The Pt/C electrodes were hot pressed at 150 °C and 10 bar (25 min) to the TPS acid-doped polymer electrolyte membrane in a dye set up using Teflon (Dupont, USA) and FEP gaskets to achieve the appropriate compression and sealing in the single cell.

The HER on the Ti electrodes was investigated by means of steady-state polarization measurements. All the tests were performed in 1M or 4,5M solution of H₂SO₄. Before the tests, the CE was washed by distilled water.

The *in-situ* electrochemical measurements were performed using a single cell purchased from Fuel Cell Technologies Inc. Both graphite bipolar plates of the single cell had the same single serpentine flow field for the distribution of reacting gases. The active area of the electrodes was 2 × 2 cm. The assembling torque applied for the single cell was 4.8 Nm. The cell was installed in a test station which was built in-house and had provisions for controlling the temperature, humidity and flow of the reacting gases. The measurements were made in a four-electrode arrangement using Autolab PGstat302.

XPS

The chemical states and composition of the layers were studied by XPS analysis. The investigations were carried out by means of a VG

Escalab Mk II spectrometer (England) using an Al K_α excitation source (1486.6 eV) with a total instrumental resolution of ~1 eV, under a base pressure of 1.10⁻⁸ Pa. The O 1s, Ce 3d, Zr 3d and Y 3d photoelectron lines were calibrated to the C 1s line. The surface composition of the mixed oxide layers was determined from the ratio of the corresponding peak areas, corrected with the photoionization cross sections.

SEM

The structure and morphology of the surface of YSZ samples were characterized by a JEM-200CX electron microscope (Japan) equipped with an ASID-3D ultrahigh resolution scanning system in the regime of secondary electron image (SEI). The accelerating voltage was 120 kV, I ~100 μA. The vacuum was ~ 1.10⁻⁶ Torr.

RESULTS AND DISCUSSION

Structural and morphological characterization of the fabricated electrodes

All of the Ti prepared electrodes were analyzed by SEM, XPS, and XRD.

XPS is a surface-sensitive spectroscopic technique that measures the elemental composition, chemical state and electronic state of the elements in the material. The data from these analyses, performed by us are summarized in Tables 1 and 2.

The XPS spectra of the thin films prove that as a result of the process of electro-deposition, the obtained layers represent a mixture of ZrO₂, Ce₂O₃/CeO₂ and Y₂O₃.

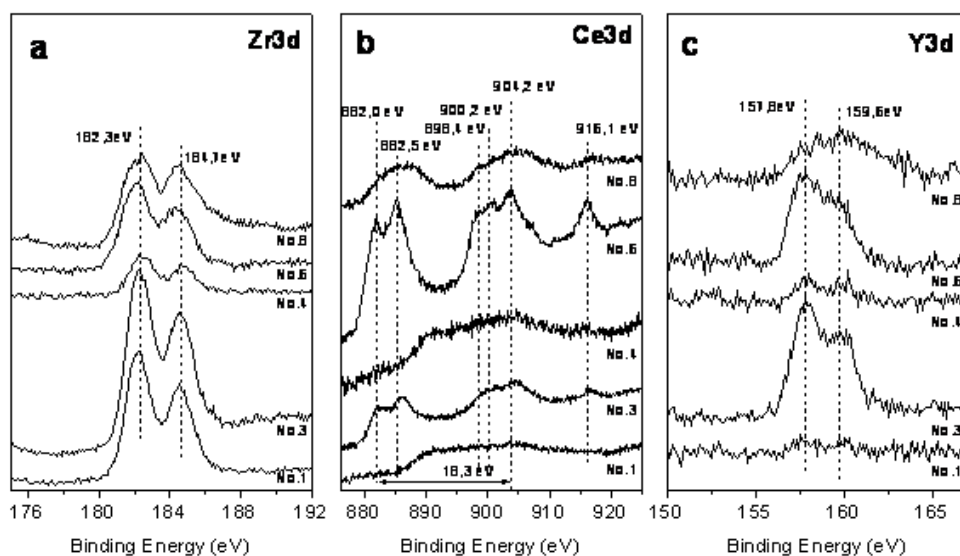


Fig 1. XPS spectra of a: Zr3d; b: Ce3d and c: Y3d.

Fig. 1a shows the Zr3d spectra. The Zr3d spectra of all samples are typical for the Zr⁴⁺ oxidation state [22, 24]. The positions of Zr3d_{3/2} and Zr3d_{5/2} are at 182.3 eV and 184.7 eV, respectively, and the distance between them is 2.4 eV.

Figure 1b shows the spectra of Ce3d. They are characterized by a complex structure, due to hybridization of the cerium ion with the ligands of oxygen orbitals and partial occupation of the valence 4f orbital [25]. As a result of this, spin-orbital splitting appears in the doublet peaks, whereupon each doublet has an additional structure, owing to the effect of the final state. Three doublets at 882.0 and 900.2 eV, respectively, 887.6 and 906.7 eV and 898.4 and 916.1 eV, can be attributed to Ce (IV), whereas the other 2 doublets, 881.1 and 899.0 eV and 882.5 and 904.2 eV, are due to Ce(III). At the same time the distance between the peaks at 882.0 eV and 904.2 eV is 18.4 eV. The spectrum of Ce III is a result from a 3d¹⁰4f⁰ final state, while the spectrum of Ce IV is a result from a 3d¹⁰4f¹ final state [26]. Hence, the XPS spectra of all samples show that ceria in all ZrO₂-CeO₂-Y₂O₃ – thin films are in the III and IV oxidation state.

Figure 1c shows the spectrum of Y3d. The peak position of Y3d_{5/2} at 157.8 eV and the distance of 1.75 eV between Y3d_{5/2} and Y3d_{3/2} peaks shows that yttrium is in an Y³⁺ - oxidation state.

The analysis of the chemical composition of the electrodeposited thin films shows that there is a strong relation between composition (ratio between Zr and Ce) of the electrolyte and the elemental amounts in the layers. With the increase of the concentration of zirconium chloride in the

electrolyte, the amount of the zirconium in the thin films increases linearly as shown in Table 1 and Fig. 2.

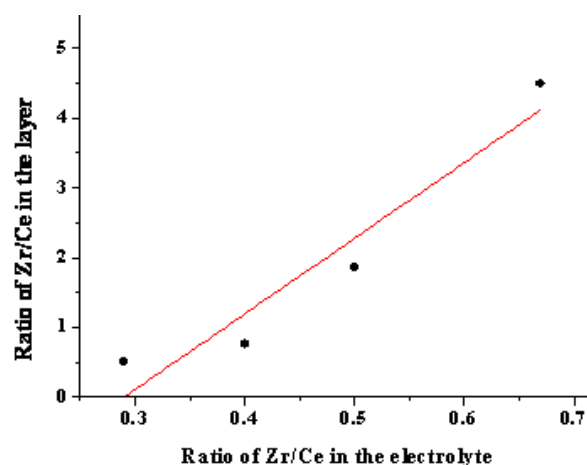


Fig. 2. Correlation between the ratio Zr/Ce in the electrolyte and after deposition on the electrode (catalytic layer (see Table 1)); for sample No. 1 – Zr/Ce in the electrolyte = 0.67 and in the layer = 4.49, for sample No. 3 – Zr/Ce in the electrolyte = 0.50 and in the layer = 1.85, for sample No. 4 – Zr/Ce in the electrolyte = 0.40 and in the layer = 0.75, for sample No. 6 – Zr/Ce in the electrolyte = 0.29 and in the layer = 0.50.

Initially the electrolysis conditions, cell voltage and time of electrolysis were optimized. Fig. 4 represents the optimization curve of the cell voltage at a constant time of electrolysis $\tau=60$ min. The figure represents the relationship between the electrode over-potential for hydrogen evolution at a chosen current density ($i=50$ mA.cm⁻²) and a cell voltage at which the catalytic films are deposited.

Table 1. XPS data of the catalytic films tested. All films were deposited at an electrolysis cell voltage of U = 9 V.

No. of sample	Concentration of ZrCl ₄ in electrolyte [g/l]	Concentration of CeCl ₃ ·7H ₂ O in electrolyte [g/l]	Concentration of YCl ₃ ·6H ₂ O in electrolyte [g/l]	Ratio of Zr/Ce in electrolyte	Amount of ZrO ₂ in layer [at%]	Amount of CeO ₂ in layer [at%]	Amount of Y ₂ O ₃ in the layer [at%]	Ratio of Zr/Ce in layer
1	40	60	40	0,67	79,1	17,6	3,2	4,49
3	40	80	40	0,50	55,4	29,9	14,7	1,85
4	40	100	40	0,40	38,0	50,4	11,6	0,75
5	40	120	40	0,33	n.d*	n.d.	n.d.	n.d.
6	40	140	40	0,29	29,2	58,6	12,2	0,50
7	40	160	40	0,25	n.d.	n.d.	n.d.	n.d.
8	40	180	40	0,22	75,7	16,1	8,3	4,70

* – not determined

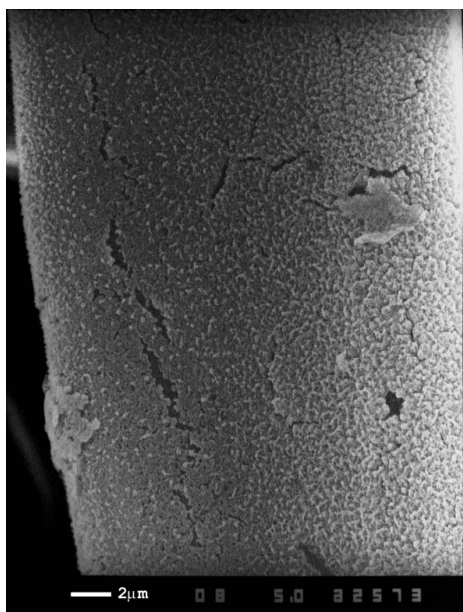


Fig. 3. SEM analysis showing the typical morphology of the electrodeposited thin films. It can be seen that the layers are smooth and with a uniform surface. There are small cracks on the surface, but in general the layers have a good adhesion

Electro-catalytic activity of the electrodes for the hydrogen evolution reaction in an aqueous electrolyte

Table 2 illustrates the dependency between the applied potential and the chemical composition of the electrodeposited layers. The sample with optimum characteristics has equal amounts of Zr and Ce.

Table 2. Chemical composition of the electrodeposited thin films, determined by XPS.

E [V]	Amount of Zr in layer [at%]	Amount of Ce in layer [at%]	Amount of Y in layer [at%]	Ratio of Zr/Ce in layer
9	-	-	-	-
12	36,0	25,5	38,4	1,41
15	43,5	41,9	14,7	1,04
18	47,7	35,6	16,7	1,34
21	33,2	41,3	25,5	0,80
24	n.d.	n.d.	n.d.	n.d.
27	n.d.	n.d.	n.d.	n.d.

Shown in Fig. 6 are the steady-state polarization curves of the best Zr & Ce & Y on Ti electrodes in 1M H₂SO₄ solution.

It is demonstrated that the best results were obtained for ZrO₂ on TiO₂ which compared with the others have the highest electro-catalytic activity, though the rest of the electrodes have close characteristics.

Shown in Fig.7 is Tafel's curve derived from Fig. 6 for an electrode with ZrO₂ on TiO₂.

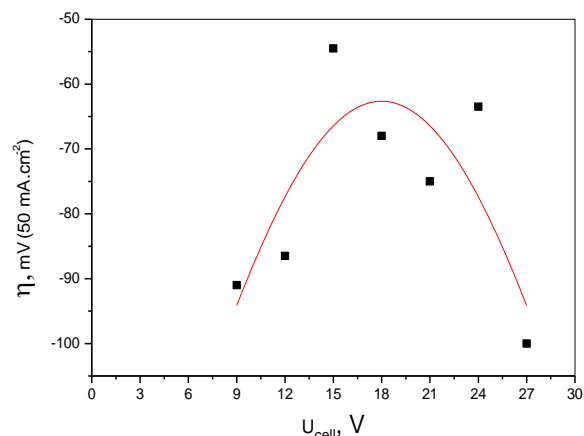


Fig. 4. Optimization curve for electrodes with catalytic films deposited at a different cell voltage. Time, τ=60 min.

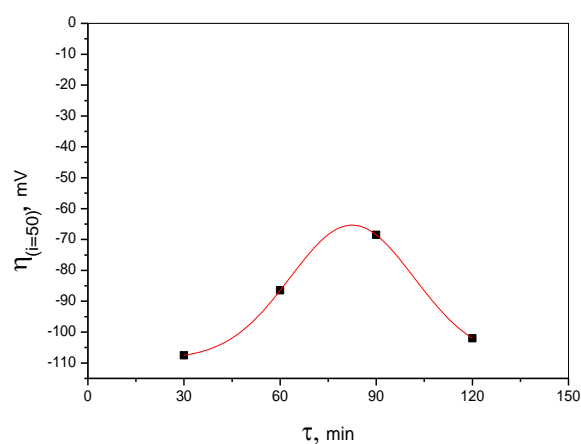


Fig. 5. Optimization curve for electrodes with catalytic films deposited for different periods of electrolysis. The cell voltage is U= 15V.

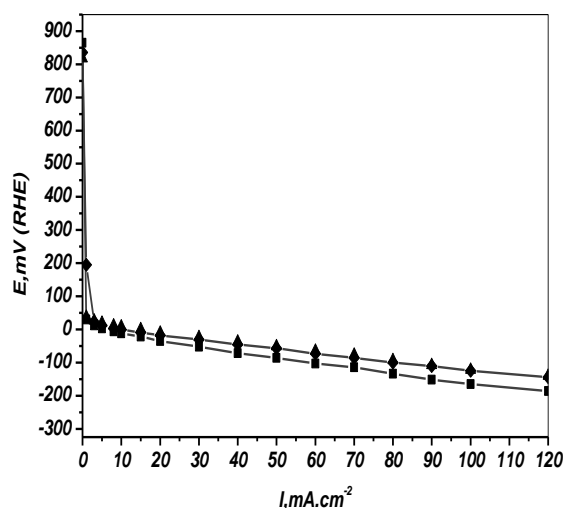


Fig. 6. Steady-state polarization curves of the Ti electrodes. ■-(Ti+Zr&Ce&Y)₁₇₄, ▲- (TiO₂_ZrO₂)₁₇₄, ◆- (Ti+Zr&Ce&Y)₁₇₅, 1M(H₂SO₄), CE(Pt).

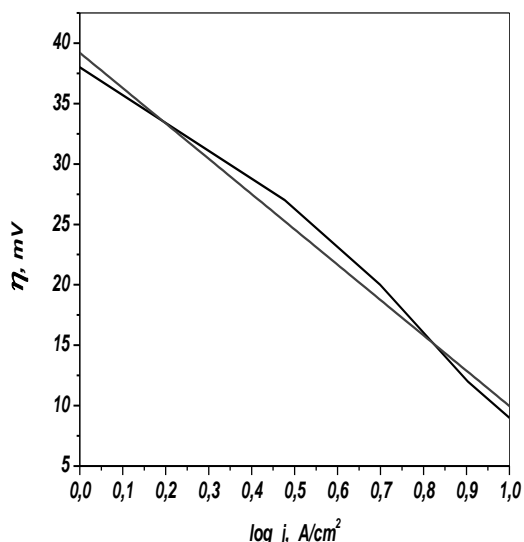
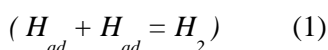


Fig. 7. Tafel's curves derived from Fig. 6.

The Tafel slope is $b \sim 30 \text{ mV}$, which is equivalent to Tafel's mechanism [27] for the electrochemical reaction:



Electro-catalytic activity of the electrodes for the hydrogen evolution reaction at elevated temperatures

Electrodes of (Zr, Y & Ce on Ti) with an optimized composition were tested with a TPS membrane at temperatures of 150 – 180°C.

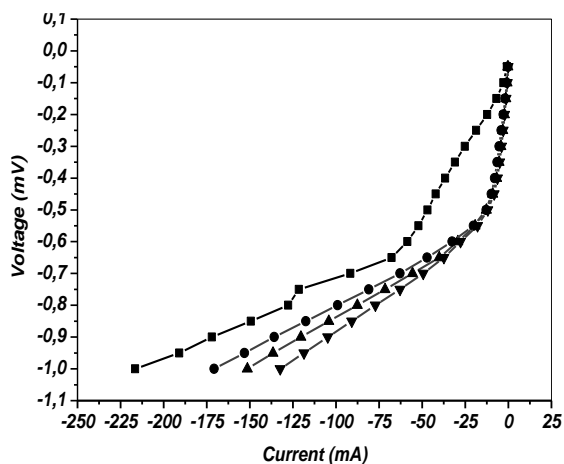


Fig. 8. VA characteristics of Zr, Y & Ce electrodes on Ti and carbon cloth at different temperatures; 150°C - ▼, 160°C - ▲, 170°C - ●, 180°C - ■.

The results confirm the activity of (Zr, Y & Ce on Ti) electrodes. Figs. 8 and 10 present the effect of temperature on the performance of MEA. Interestingly, the performance drops with increasing temperature and the main feature of the MEA behavior is the appearance of a diffusion limited performance at elevated temperatures. This

may be caused by a decrease of the membrane's proton conductivity due to the decrease of the hydration level of the MEA at elevated temperatures. Also the increase in temperature may lead to a decrease in the hydration level of H₃PO₄ in the catalytic layer which is responsible for the development of the electrochemical interface and the establishment of the ionic link between the electro-catalyst and the polymer electrolyte. Also the steam supplied can absorb in the H₃PO₄ layer and may cause a reduction in performance as steam can be a limiting reactant.

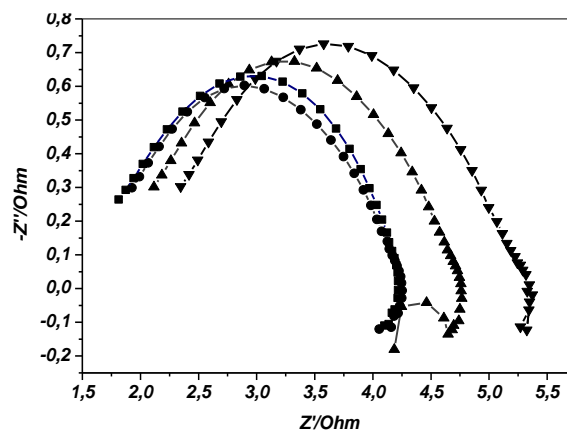


Fig. 9. Impedance spectra of Zr, Y & Ce on a Ti electrode (from Fig. 7) at different temperatures. 150°C - ▼, 160°C - ▲, 170°C - ●, 180°C - ■.

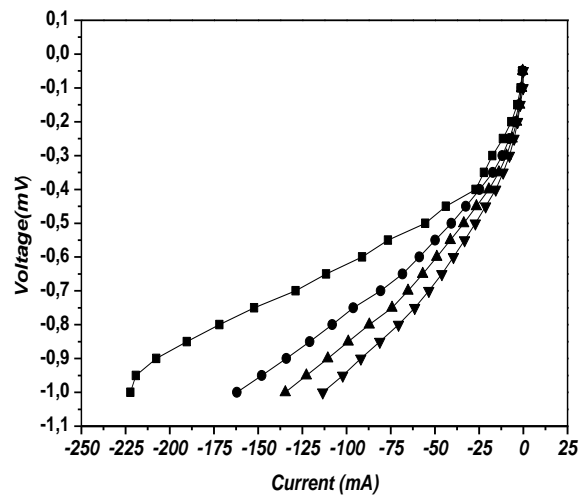


Fig. 10. I-V characteristics of ZrO₂ on a Ti electrode and carbon cloth at different temperatures: 150°C - ▼, 160°C - ▲, 170°C - ●, 180°C - ■; Electrode – PBI membrane.

An increase in the impedance with temperature reduction is clearly apparent. The impedance spectra of the tested electrodes with the increase in temperature show a decrease in the reaction resistance. Impedance measurements can be utilized to help select the right material suitable for electrochemical applications [28].

As known, the polarization phenomena at the electrode-electrolyte interface play a key role in cell behavior [29].

CONCLUSIONS

Ti electrodes were prepared as cathode materials for hydrogen evolution reactions. Our experiments revealed a Tafel recombination mechanism where the nature of the hydrogen evolution process coincides precisely with the original recombination theory proposed by Tafel back in 1905 and is similar to that observed for other metals such as platinum.

The steady-state polarization curves, Tafel curve and SEM, XPS and XRD were used to evaluate the hydrogen evolution process. The optimized electrodes have shown high electro-catalytic activity both in liquid acid and with TPS membranes at temperatures 150 – 180°C.

REFERENCES

1. Catalysis by Ceria and Related Materials, World Scientific – Imperial College Press, London, 2002.
2. S. Trasatti in *Electrocatalysis of Hydrogen Evolution: Progress in Cathode Activation - ADVANCES IN ELECTROCHEMICAL SCIENCE AND ENGINEERING*, H. Gerischer, C.W. Tobias (eds), Vol.2, 2008, p.1
3. L. Brewer, *The cohesive energies of the elements*, LBL-3720, Berkeley, California, 1977.
4. M. M. Jaksic, C. M. Lacnjevac, B. N. Grgur, N. V. Krstajic, *J. New Mat. Electrochem. Systems*, **3**, 169 (2000).
5. N.A. Galaktionova, *Hydrogen in Metals*, Metalurgiya, Moscow, 1967.
6. A. Trovarelli, C. De Leitenburg, M. Boaro, G. Dolcetti, *Catal. Today* **50**, 353 (1999).
7. D. Duprezand, C. Descome, in: *Catalysis by Ceria and Related Materials*, World Scientific – Imperial College Press, London, 2002, p. 243.
8. US **7,824,574 B2**, (2010).
9. A. Hauch, S. D. Ebbesen, S. H. Jensen, M. Mogensen, *J. Mater. Chem.*, **18**, 2331 (2008).
10. M. Pilar Yeste, Juan C. Hernandez-Garrido, D. C.Arias, G.Blanco, J.M. Rodriguez-Izquierdo, J.M. Pintado, S. Bernal, J.A. P. Omiland, J.J. Calvino, *J. Mater. Chem. A*, **1**, 4836 (2013).
11. J. Matthiesen, S. Wendt, J. Ø. Hansen, G. K. H. Madsen, E. Lira, P. Galliker, E. K. Vestergaard, R. Schaub, E. Lægsgaard, B. Hammerand, F. Besenbacher, *ACS Nano*, **3**(3), 517 (2009). [<http://pubs.acs.org/cgi-bin/cen/trustedproxy.cgi?redirect=http://pubs.acs.org/doi/abs/10.1021/nn8008245>].
12. National Academy of Engineering, *The Hydrogen Economy: Opportunities, Costs, Barriers, and R&D Needs*, Washington, D.C.: The National Academies Press, 2004.
13. BMW Group Clean Energy ZEV Symposium. September, (2006).
14. EPA mileage estimates. Honda FCX Clarity - Vehicle Specifications. American Honda Motor Company, 2010.
15. Fuel Cells: Cost, California Distributed Energy Resource Guide. California Energy Commission, 2002.
16. A.T. Marshall, S. Sunde, M. Tsytkin, R. Tunold, *Int. J. Hydrogen Energy*, **32**, 2320 (2007).
17. V. Baglio, A. Di Blasi, T. Denaro, V. Antonucci, A.S. Aricò, R. Ornelas, F. Matteucci, G. Alonso, L. Morales, G. Orozco, L.G. Arriaga, *J. New Mater. Electrochem. Syst.*, **11**, 105 (2008).
18. V. Antonucci, A. Di Blasi, V. Baglio, R. Ornelas, F. Matteucci, J. Ledesma-Garcia, *Electrochim. Acta*, **53**, 7350 (2008).
19. Q. Li, J.O. Jensen, R.F. Savinell, N.J. Bjerrum, *Prog. Polym. Sci.*, **34**, 449 (2009).
20. S.A. Grigoriev, P. Millet, S.A. Volobuev, V.N. Fateev, *Int. J. Hydrogen Energy*, **34**, 4968 (2009).
21. M. Geormezi, C.L. Chochos, N. Gourdoupi, S.G. Neophytides: J.K. Kallitsis, *Journal of Power Sources*, **196**, 9382 (2011).
22. J.H. Scofield, *J. Electron. Spectrosc. Rel. Phenom.*, **8**, 129 (1976).
23. A.M. Ginberg, *Galvanotechnika, Metallurgia Publ. H.*, 1987, p.87.
24. *Handbook of X-ray Photoelectron Spectroscopy*, second ed., Perkin-Elmer Corporation, Eden Prairie, MN, 1992.
25. X. Yu, G. Li, *Journal of Alloys and Compounds*, **364**, 193 (2004).
26. J.M. Sánchez-Amaya, G. Blanco, F.J. Garcia-Garcia, M. Bethencourt, F.J. Botana, *Surface & Coatings Technology*, **213**, 105 (2012).
27. Y. Gerasimov, *Physical Chemistry*, Vol. 2, MIR Publishers, Moscow, 1985, p.581.
28. N. B. Beekmans, L. Heyne, *Electrochim Acta*, **21**, 303 (1976).
29. S.P.S. Badwal and H. J. De Bruin, *Phys. Stat. Sol. (a)*, **54**, 261 (1979).

ЦИРКОНИЙ, ЦЕРИЙ И ИТРИЙ ВЪРХУ КАТОДИ ОТ ТИТАН ПРИ ПОЛУЧАВАНЕ НА H₂ В КИСЕЛ ЕЛЕКТРОЛИТ

С. Восканян¹, А. Цанев¹, Н. Шроти², Г. Пчеларов¹, К. Петров^{1*},

¹ *Институт по електрохимия и енергийни системи – БАН
ул. Акад. Г. Бончев бл. 10, 1113 София, България*

² *Департамент по инженерна химия, Университет в Патрас, GR 26504 Патрас, Гърция*

Получена на 16 декември 2014 г.; коригирана на 20 май 2015 г.

(Резюме)

Изследвани са катализатори за получаване на водород на базата на Zr, Ce, Y сплави. Електродите са получени чрез електрохимично отлагане на сплавите от разтворите ZrCl₄, CeCl₃·7H₂O и YCl₃·6H₂O върху мрежа от титан. Реакцията на отделяне на водород беше изследвана в кисели разтвори: 1M или 4.5 M H₂SO₄ (течност) и РВІ мембрани с фосфорна киселина при стайни и високи температури. Морфологията и микроструктурата на електродите са характеризирани със сканиращ електронен микроскоп и X-ray дифракция. Електрокаталитичната активност е определена с помощта на поляризационни криви, Тафелови наклони и електрохимична импедансна спектроскопия. Показано е, че електрокаталитичната активност на изработените електроди зависи от морфологията и микроструктурата на порьозния електрод. Той има ниско съпротивление на пренос на заряд и висока плътност на обменния ток. Измерена е висока електрокаталитична активност в температурния интервал – 25° до 160°C.